Journal of the Brazilian Society of Mechanical Sciences and Engineering (2021) 43:178
https://doi.org/10.1007/s40430-021-02895-9

TECHNICAL PAPER

Microstructure and mechanical properties of the bonded interface of laser impact welding brass/SS304

Feng Li[1] · Xiao Wang[1] · Meng Shao[1] · Xiaojun Wang[1] · Jiaxin Lu[1] · Huixia Liu[1]

Received: 18 May 2020 / Accepted: 13 February 2021 / Published online: 4 March 2021

Abstract

In this study, laser impact welding experiments on H62 brass and stainless steel 304 (SS304) were carried out, the feasibility of welding the two alloys was analyzed, and the influences of laser energy and flyer plate thickness on the surface morphology and interface waveform of the welded joint were studied. The elemental distribution of the welding interface was measured and examined. The mechanical properties of the welded sample were also systematically explored. Results show that weldability between the flyer and the substrate plate at a flight distance of 0.2 mm is the best when the other process parameters are the same. When the thickness of the flyer plate is constant, the amplitude and wavelength of the bonding waveform decrease as laser energy decreases. Under the same laser energy, the amplitude and wavelength of the interface waveform decrease as flyer plate thickness increases. Energy-dispersive spectroscopy results reveal an approximately 6 μm-thick element diffusion layer at the bonding interface. Two failure types occur in tensile shear failure: bonding interface peeling failure and bonding edge fracture failure. The maximum force decreases sharply under excessive laser energy or flight distance. The connection strength decreases as the flyer plate thickness decreases.

Keywords High-speed impact welding · Interface waveform · Element diffusion · Local thinning · Tensile shear test

1 Introduction

In the modern industry, brass has become an indispensable material in economic development due because of its good thermal conductivity, electrical conductivity, and excellent formability. Its wear resistance and corrosion resistance are better than those of pure copper, so it has been widely used in aviation, chemical industry, and energy industry [1]. However, in some occasions in which a high strength connection is needed, a single brass material hardly meets application requirements because of the poor strength of brass. Stainless steel, which has high strength and toughness, is commonly used. Brass and stainless steel dissimilar metal welding structures are becoming more and more extensive, such as cooling pipes in refrigeration equipment, automobile heat exchangers, synchronizer cone rings, reducer turbines and bearings. However, traditional welding methods are prone to melting and cracks in the welding process, resulting in the low connection strength of welded joints [2–4]. Therefore, an appropriate welding process should be explored to achieve the effective bonding of brass and stainless steel.

Solid-phase welding does not produce large-scale melting and can avoid the formation of defects, such as heat-affected zones and cracks. As such, this process is especially suitable for bonding between dissimilar metals. Moreover, the bonding interface strength of a welding specimen is usually not less than the strength of original materials. At present, the solid-phase welding method for brass and stainless steel is limited to explosive welding and friction stir welding. In 2011, Wronka et al. [5] studied the explosive welding and bonding mechanism of brass and stainless steel. In 2012, Luo et al. [6] used friction stir welding to obtain a connection between brass and stainless steel. Their experimental results show that their welding sample has a good bonding quality, and elemental diffusion occurs at the welding interface. In 2013, Kimura et al. [7] achieved the friction stir welding of brass and stainless steel. When exploring the welding process parameters, they found that the joint strength of the welded sample of brass and stainless steel improves under

Technical Editor: Izabel Fernanda Machado.

✉ Xiao Wang
wx@ujs.edu.cn

[1] School of Mechanical Engineering, Jiangsu University, Zhenjiang 212013, China

suitable process parameters. In 2016, Bai et al. [8] applied explosive welding to establish the connection of brass and stainless steel and systematically explored the mechanical properties and microstructure of welded samples. Gao et al. [9] realized friction stir welding between brass and stainless steel and focused on the influences of welding velocity on the mechanical properties and microstructure of welded joints. Therefore, friction stir and explosive welding can result in an effective connection between brass and stainless steel, but these two welding methods have disadvantages. In explosive welding, a flyer plate is pushed to generate impact with a substrate plate via an explosion, which produces loud noise during welding, and explosive welding is not suitable for micro-welding. In friction stir welding, process parameters, such as rotation speed of a stirring rod and welding speed, should be strictly adjusted, and the wear of the stirring rod should be considered. As such, this welding process is complicated. Angshuman et al. [10] analyzed the influence of process parameters on weld performance by discussing the advantages and limitations of magnetic pulse welding (MPW). In addition, their research analysis also provides good suggestions for the future research direction of MPW. However, their research and analysis of the current MPW also has limitations in design and process.

In recent years, laser impact welding (LIW), as a new type of solid-phase welding technology, is not limited by the melting point and thermal expansion coefficient of materials. It is simple, easily controlled, and suitable for microwelding between dissimilar materials. It also has a high degree of automation, so it has gradually attracted the attention of researchers. In 2011, Zhang et al. [11] welded Al/Fe via LIW and showed that the bonding interface of the welded joint is smoother than that of explosive welding or magnetic pulse welding. In 2014, Wang et al. [12] successfully created a connection of the same metal Al/Al and the dissimilar metal Al/Cu by using an angle LIW process. In 2015, Wang et al. [13] optimized this welding process by comparing the pit height formed by a compound plate after they selected laser shock, polycarbonate plate, black lacquer, and double-sided tape as constraining, absorbing, and linking layers of the welding system, respectively. In 2016, Wang et al. [14] formed an Al/Ti connection via LIW. The thicker the flyer plate is, the smaller the impact velocity will be under the same laser pulse energy. Liu et al. [15] proposed a new laser shock spot welding process, which performs a bulge in the position where the flyer plate is to be welded to provide the flyer plate with a certain flight distance and impact angle. In 2017, Wang et al. [16] successfully welded a wire and a metal plate via laser indirect impact welding, which expands the application range of LIW. In 2018, Liu et al. [17] successfully welded a three-layer Cu/Al/Cu plate via LIW and verified the feasibility of LIW for three-layer plates. They observed that bonding area increases as the laser pulse energy increases. The research status of LIW technology shows that this solid phase welding process can weld dissimilar metals and alloys very well, which provides a new idea for the welding of brass and SS304. However, the physical and chemical properties such as density, melting point, and hardness of brass and SS304 determine that brass and SS304 are more difficult to weld than pure metal. Therefore, it is necessary to study the welding mechanism, welding process, and the interaction of welding materials between brass and stainless steel.

In this study, LIW provided a new way for micro-welding of Brass/SS304, and the influences of laser energy, flight distance, and thickness of the flyer plate on the welding process of the two alloys were analyzed. The surface morphology and cross-sectional morphology of welded samples with different laser pulse energies and thicknesses of the flyer plate were observed using an optical microscope. The microstructure of the bonded interface was examined using a scanning electron microscope (SEM), and the influences of laser pulse energy and thickness of the flyer plate on the microstructure of the bonded interface were explored. The elemental diffusion of the bonding interface was analyzed via energy-dispersive spectroscopy line scanning. The effects of different laser pulse energies, flight distances, and thicknesses on the maximum force were investigated via a tensile shear test, and failure mode was evaluated under various welding conditions.

2 Mechanism of LIW

The principle of LIW is shown in Fig. 1. The welding system comprises a focusing lens, a blank holder, a constraining layer, a flyer plate, an ablative layer, a substrate plate, and a back support. Polymethyl methacrylate has good impact resistance and light transmittance, which are selected as the constraining layer in the experiment. When the pulse laser irradiates on the ablative layer through the transparent constraining layer through the focusing lens, the ablative layer (black paint) quickly vaporizes and ionizes into plasma under the irradiation of the pulse laser. The plasma expands rapidly after it absorbs the laser pulse energy because of the limitation of the constraining layer, thus forming a strong shock pressure wave on the surface of the flyer plate [18]. Under the influence of a shock wave, the flyer plate flies downward at a high speed to achieve impact welding.

Figure 2 shows a schematic of LIW [19]. The flyer plate is placed parallel to the substrate plate before welding with a certain flight distance, as shown in Fig. 2a. The beam induces a quasi-Gaussian shock wave, and the flyer plate protrudes downward and accelerates to fly downward under the action of the shock wave, as shown in Fig. 2b. When the flyer plate is accelerated by a certain distance,

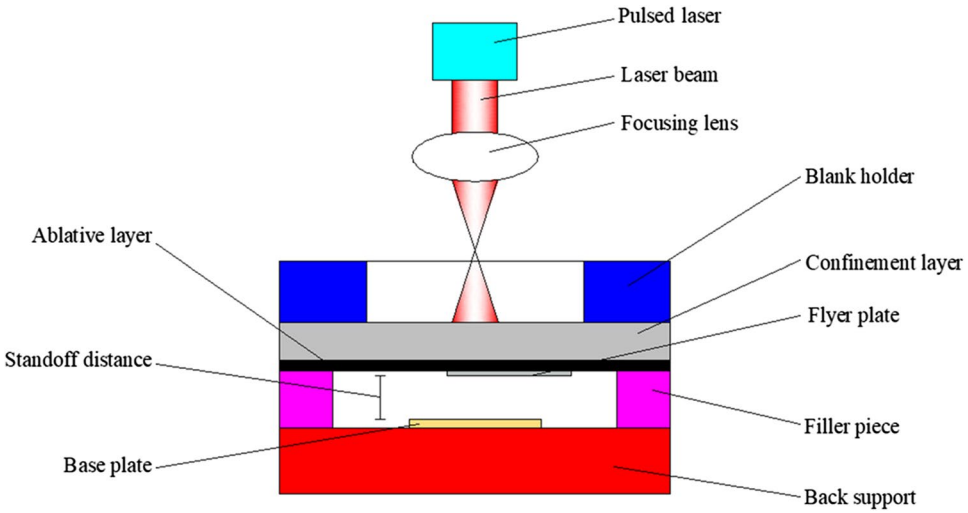

Fig. 1 Mechanism of LIW

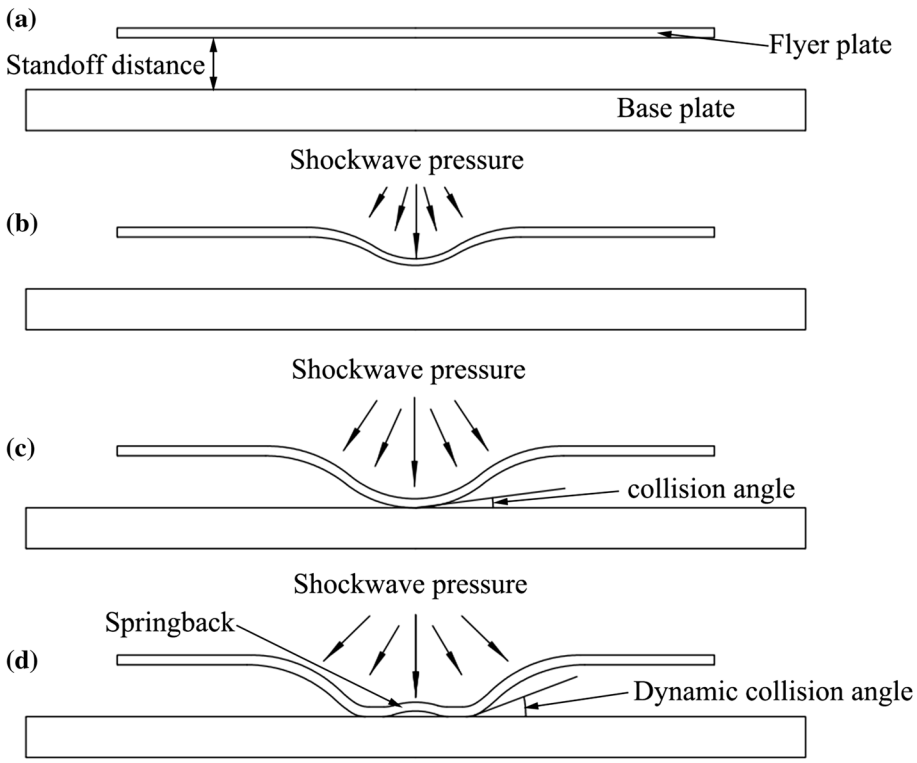

Fig. 2 Schematic of LIW process [19]: **a** initial placement; **b** flyer plate bulge; **c** impact angle between the flyer and substrate plates; and **d** springback phenomenon

as shown in Fig. 2c, the convex portion of the center of the flyer plate first collides with the substrate. Theoretically, the impact angle between the flyer and the substrate plate is 0° at the beginning stage of the welding, and the impact angle does not reach the critical angle necessary for welding. Therefore, the flyer and the substrate plate are not welded. With the progress of the welding process, the impact angle increases gradually. Only when the shock angle approaches the necessary critical angle, a jet is produced between the flyer and the substrate plate, and the solid-phase metallurgical bonding is achieved. Intermediate unwelded areas form during welding, as shown in Fig. 2d because the impact angle is small, and the critical angle is not reached at the beginning stage of welding. Upon striking the substrate, the flyer plate generates a downward shock wave. According to the principle of shock wave propagation, the reverse shockwave corresponding to the same is generated on the flyer plate at the moment of collision [20]. When the reverse impact stress on the flyer plate exceeds the plastic deformation limit of the flyer plate material, the flyer plate forms an upward bending bulge, resulting in a springback phenomenon.

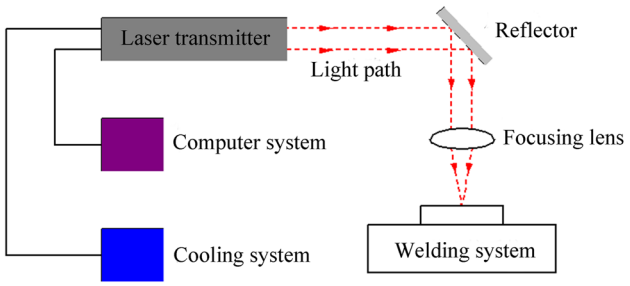

Fig. 3 Laser high-speed impact welding experimental system

Springback is disadvantageous for LIW, which increases the intermediate unwelded area.

3 Experimental preparation

3.1 Experimental equipment

The LIW experimental system used in this study is shown in Fig. 3. It is mainly composed of a computer control system, a laser transmitter, a cooling system, and a workpiece welding system. A Spitlight 2000 Nd:YAG laser was used in the experiment. Table 1 shows the main parameters of Spitlight 2000 Nd:YAG laser. A KEYENCE VHX-1000C ultra-depth of field three-dimensional microscope was utilized to survey the surface morphology and cross-sectional morphology of welding specimens at magnification ranging from 20× to 5000×. The operation is convenient, and the observation results are reliable. An S-3400 N SEM was used to observe the microstructure of the welded cross section and analyze the elemental diffusion, especially to observe the formation of the interface waveform and the jet and to conduct point, line, and area scanning of the elements near the welding interface. A universal testing machine with a maximum range of 10 kN and a load resolution of 0.01 N was utilized to examine the welding sample via a tensile shear test.

Table 1 Main parameters of Spitlight 2000 Nd:YAG Laser

Experimental parameters	Value
Laser wavelength	1064 nm
Pulse width	8 ns
Exit spot diameter	9 mm
Energy stability	$< \pm 1\%$
Laser pulse energy	80–1800 mJ

3.2 Experimental parameters

The flyer and substrate plate materials in this experiment were H62 brass and SS304, respectively. With the rapid development of electronic products, biology, medical devices, precision instruments, sensors, and other industries, the miniaturization, precision, and high performance of products has become one of the important trends in the development of manufacturing industry, which promotes the research of micro-welding technology. Therefore, the flyer plate was cut into a rectangle with dimensions of 20×5 mm, and the substrate plate was cut into a square with dimensions of 20×20 mm. The chemical compositions of H62 brass and SS304 are shown in Tables 2 and 3, respectively. In addition, a spot diameter of 1.5 mm was used in the experiment. Laser pulse energies of 565, 835, 1200, 1550, and 1800 mJ and flyer plate thickness values of 0.01, 0.02, 0.03, and 0.04 mm were selected. The thickness of the substrate plate was 0.08 mm. Three different flight distances of 0.1, 0.2, and 0.3 mm were used. The flight distance is related to the critical impact angle [21] and impact velocity [22]. The experimental parameters and experimental conditions are presented in Table 4.

4 Results and discussion

4.1 Surface morphology and cross-sectional morphology of welded samples

At a flight distance of 0.2 mm, the effect of laser energy on the surface and cross-sectional morphologies of the welded samples was investigated. Secondly, the influence of the flyer plate thickness on the cross section and surface morphologies of the welded specimen was investigated by keeping the laser pulse energy unchanged.

Table 2 Chemical constituents of H62 brass (wt%)

Constituents	Cu	Zn	Fe	Bi	Sb	Pb	P
Brass	61.79	37.8	0.15	0.02	0.009	0.075	0.01

Table 3 Chemical constituents of SS304 (wt%)

Constituents	Fe	Ni	Cr	Si	Mn	S	P	C
SS304	70	9	18	1	2	0.03	0.045	0.08

Table 4 Specific experimental parameters

Experimental parameters	Value
Welding material	Brass/SS304
Flyer size (mm)	20×5×0.02/0.03/0.04
Substrate size (mm)	20×20×0.08
Laser pulse energy (mJ)	565, 835, 1200, 1550, 1800
Flight distance (mm)	0.1, 0.2, 0.3
Spot diameter (mm)	1.5

Figure 4a and b shows the surface morphology of the welding specimen under 1200 and 1800 mJ, respectively. Obvious ripples can be observed on the surface of the flyer plate when the laser pulse energy is 1800 mJ, whereas when the laser pulse energy is 1200 mJ, the surface of the weldment is flat, and no ripples appear. This finding is mainly due to the different impact speed of the flyer plate. Under the laser pulse energy of 1800 mJ, the flyer plate can obtain a high impact velocity, resulting in more serious plastic deformation, thus forming surface ripples. Figure 4c shows the surface morphology of the flyer plate with a thickness of 0.04 mm under the laser pulse energy of 1800 mJ. The welding surface is flat and smooth, which is similar to that shown in Fig. 4a. The thicker the flyer plate is, the smaller the impact velocity will be. At a low impact velocity, the degree of the plastic deformation of the flyer panel is relatively reduced. Hence, the surface morphology of the welding specimen is relatively flat.

Figure 5 shows the cross-sectional morphology of the welding samples, specifically the intermediate unwelded areas. Hence, the effective welded area of brass and stainless steel is the annular area. Figure 5a and b presents the jet formation, which is a necessary condition for successful high-speed shock welding. Figure 5a and b illustrates the cross-sectional morphologies of different laser beam energies at the same flyer plate thickness (0.02 mm). The comparison of the cross-sectional figures of the welding specimen under the two laser pulse energies reveals that the intermediate unwelded area decreases as the laser energy decreases. The increase in laser energy also increases the impact velocity at the edge of the impact region, resulting in a wider range of thee plastic deformation of the flyer plate. Thus, the diameter of the outer circle of the weld region increases. The area of the effective weld zone eventually increases because the increase rate of the outer circle diameter of the weld zone is greater than the diameter of the intermediate unwelded zone. Liu et al. [15] observed a similar phenomenon when studying a new type of LIW process. Figure 5c shows a cross-sectional optical micrograph of a welded specimen with a flyer plate thickness of 0.04 mm at a laser pulse energy of 1800 mJ. The unwelded area in the middle slightly changes compared with brass with a thickness of 0.02 mm possibly because the impact energy obtained by the flyer plate is substantially the same. As such, the impact of the rebound on the area of the intermediate unwelded region is slightly different. However, the diameter of the outer circle of the welding area decreases obviously because the thicker the compound plate is, the more difficult the production of plastic deformation will be. The plastic deformation range of the thicker flyer plate during impact welding is small under the same laser pulse energy, resulting in a rapid decrease in the diameter of the outer circle of the welding area. The increase in the thickness of the flyer plate reduces the impact velocity at the edge of the impact region. Consequently, achieving a range of effective impact velocities is difficult. This condition may also explain the decrease in the diameter of the outer circle of the weld region. The area of the effective weld area decreases as the thickness of the flyer plate increases.

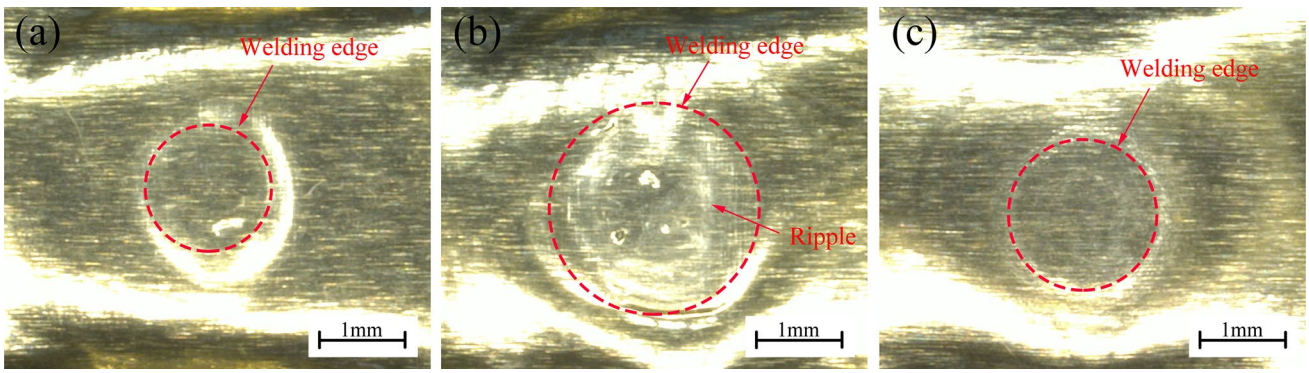

Fig. 4 Surface topography of welding samples (standoff distance: 0.2 mm): **a** flyer plate thickness of 0.02 mm and laser pulse energy of 1200 mJ; **b** flyer plate thickness of 0.02 mm and laser pulse energy of 1800 mJ; and **c** flyer plate thickness of 0.04 mm and laser pulse energy of 1800 mJ

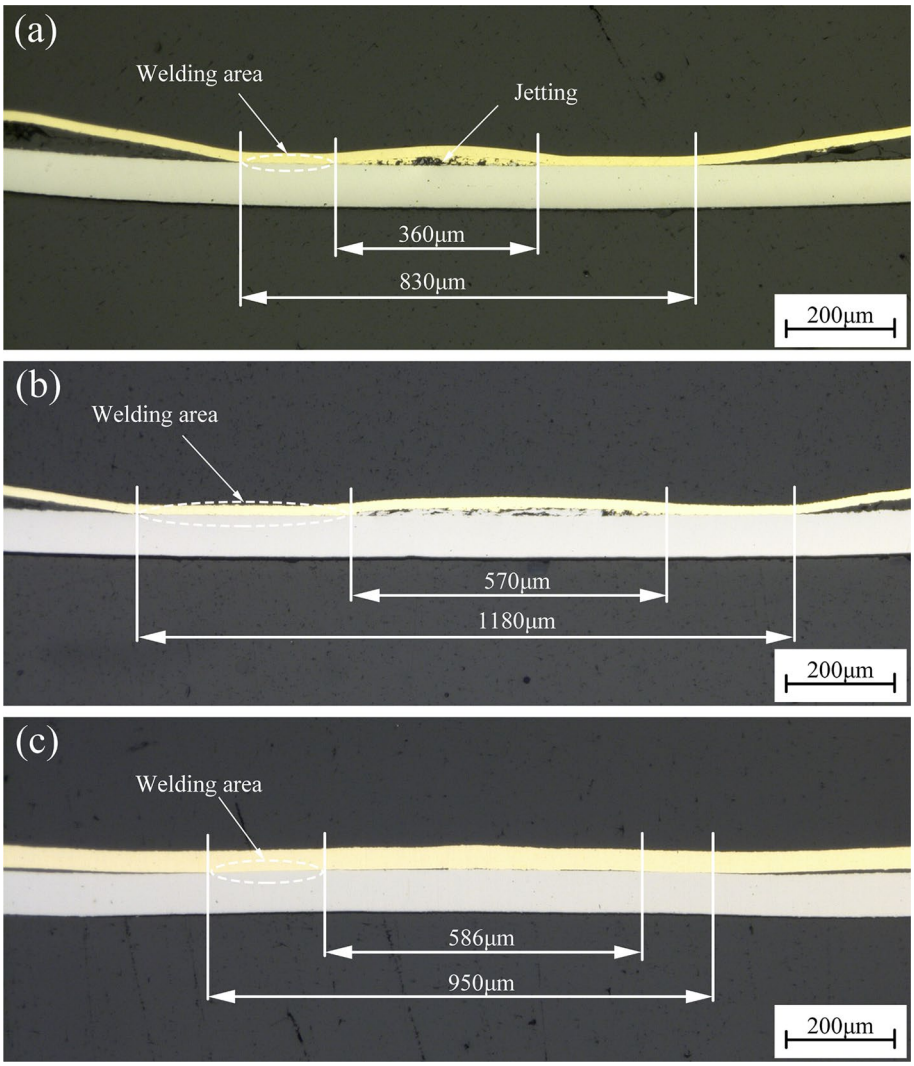

Fig. 5 Cross-sectional morphology of the welding samples (standoff distance: 0.2 mm): **a** flyer plate thickness of 0.02 mm and laser pulse energy of 1200 mJ; **b** flyer plate thickness of 0.02 mm and laser pulse energy of 1800 mJ; and **c** flyer plate thickness of 0.04 mm and laser pulse energy of 1800 mJ

4.2 Effect of laser pulse energy and flyer plate thickness on the microstructure of bonding interface

Figure 6 shows the microstructure of the bonded interface of the welded samples at pulses of 835, 1200, 1550, and 1800 mJ at a flying distance of 0.2 mm. As shown in Fig. 6, no obvious melting was found at the welding interface. However, we found that welding interface will produce obvious melting phenomenon when the laser energy is too large in our previous research [19]. The bonding interface is flat at a laser energy of 835 mJ. When the laser energy gradually increases, the bonding interface initially becomes a microwave-like interface and subsequently an obvious wavy form interface appeared. The amplitude and wavelength of the interface wave reach the maximum at a laser energy of 1800 mJ. An increase in laser energy increases the kinetic energy of the flyer plate. According to the kinetic energy theorem, the impact force of the flyer plate upon hitting the substrate also increases. An increase in the impact force increases the shear stress and impact pressure at the collision point, resulting in a more severe plastic deformation of the flyer plate and the substrate at the bonding interface and in an increase in the waveform size of the bonding interface. As discharge voltage increases, the bonding interface slowly changes from a straight line to a regular wave, and the waveform size continuously increases. Kahraman and Gülenç [23] conducted an explosion welding study and observed that the amplitude and wavelength of the combined interface waveform decrease as the explosion load decreases. Angshumanet al. [10] found a similar phenomenon in the process of analyzing MPW.

The thickness of the flyer plate is another important factor affecting the microscopic morphology of the bonded interface. Under a flight distance of 0.2 mm and a laser energy of 1800 mJ, the effects of three kinds of flyer plates with different thickness values on the microstructure of the bonding interface are investigated. Figure 7 presents the specific

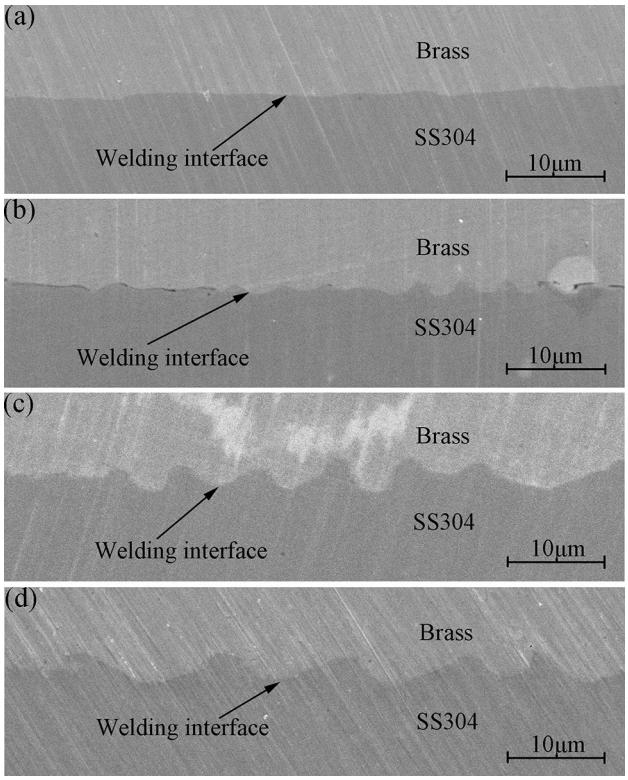

Fig. 6 Micro-morphology of the bonding interface at different laser pulse energies (standoff distance, 0.2 mm; flyer plate thickness, 0.02 mm): **a** 835 mJ; **b** 1200 mJ; **c** 1550 mJ; **d** 1800 mJ

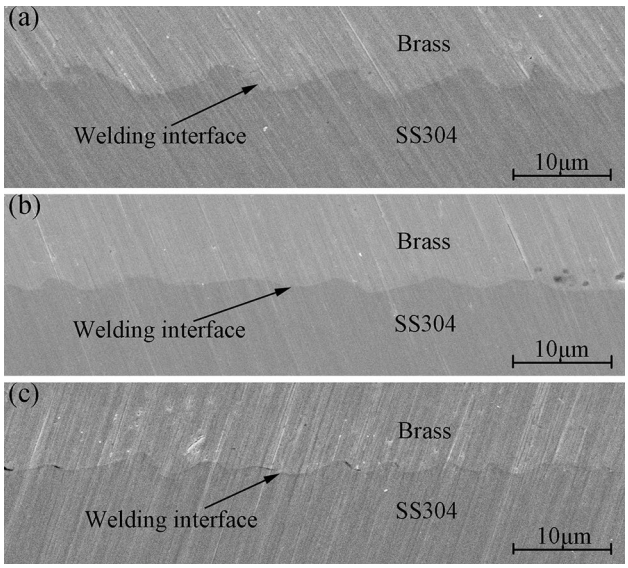

Fig. 7 Micro-morphology of the welding interface at different flyer plate thicknesses (standoff distance of 0.2 mm and laser pulse energy of 1800 mJ): **a** 20 μm, **b** 30 μm, and **c** 40 μm

microstructure. Figure 7a–c shows the welding interface morphologies of 0.02-mm-, 0.03-mm-, and 0.04-mm-thick brass and stainless steel after impact welding, respectively. The flyer plates with different thickness can obtain a good bonding interface. This result indicates acceptable welding quality. When the thickness of the brass is increased to 0.03 mm, the amplitude and wavelength of the interface waveform decrease. When 0.04-mm-thick brass is used as a flyer plate, a small and dense microwave interface is obtained. The experimental results show that the amplitude and wavelength of the interface waveform decrease as the thickness of the flyer plate increases. The reasons supporting this finding are as follows. First, an increase in the flyer plate thickness reduces the impact velocity when the flyer plate and the substrate collide, resulting in a smaller degree of plastic deformation at the interface between the flyer plate and the substrate. Second, the protruding degree of the flyer plate with different thickness differs after it receives the same impact force. The thicker the flyer plate is, the less obvious the bulge will be. Hence, the rate of change in the dynamic impact angle decreases. When the impact point moves at the same distance along the welding direction, the shock angle obtained is smaller than that of the thinner flyer plate. Therefore, the amplitude and wavelength of the bonding interface decrease as the flyer plate thickness increases under the effects of shock speed and shock angle. Manikandan et al. [24] studied the underwater explosion welding of copper and molybdenum and found that the amplitude and wavelength of the interface wave decrease when the thickness of the flyer plate increases from 0.1 to 0.3 mm. In addition, the bonding interface obtained after the flyer plates are welded with three kinds of thickness is wavy, and no straight interface wave is observed because the kinetic energy obtained by at a larger laser pulse energy is still greater than the kinetic energy obtained at a low pulse energy, although the increase in the thickness of the flyer plate reduces the impact velocity. Consequently, no flat waveform appears. Figure 7a–c shows that the interface waveforms generated are not completely symmetrical during welding possibly because of the different densities of brass and stainless steel. Chen et al. [25] also found this asymmetric wavy interface on the explosive welding of aluminum and magnesium alloys. Akbari et al.[26] investigated the explosion welding of titanium and stainless steel and observed that waveform asymmetry is due to the difference in density between different materials. In addition, higher the flyer thickness, higher is the requirement of kinetic energy for deformation. When the thickness of the flying board increases, and the laser energy remains the same, this may result in insufficient welding energy, so the left side of Fig. 7c may be that the connection is not good

enough. Meanwhile, the surface impurities may be removed by the jet to the outside of the welding environment.

In the experiment, whether it is changing the loaded laser energy or changing the thickness of the flyer plate, in fact, the main influence is the impact velocity between the flyer plate and the substrate. The larger the shock velocity is, the larger the waveform size of the interface wave will be. The impact angle has a certain influence without changing the flight distance, but the degree of influence is small. The main factor affecting the waveform size of the bonding interface is shock speed.

4.3 Interface element analysis

The acceleration voltage, resolution, and spot size used in EDS scanning are 15kv, x3k, and 50 nm, respectively. The EDS line scan analysis of the brass/SS304 interface is illustrated in Fig. 8. The black line segment is the position where the EDS line is scanned as shown in Fig. 8a. The brass/SS304 bonding interface line scan results are presented in Fig. 8b, where the black and red curves represent the trends of the main elements (i.e., Fe and Cu) of the two alloys, respectively. Fe starts to rise significantly at approximately 4 μm from the initial position of the line scan. When the line scanning position is 0.01 mm, Fe increases to a steady stage, whereas Cu decreases sharply in this range. Hence, the element diffusion layer thickness is approximately 6 μm. High pressure and temperature occur upon impact, so elemental diffusion at the interface is inevitable [27]. However, the LIW time is very short, and it does not form a sufficiently high pressure and temperature condition similar to that in diffusion welding. As such, a very thick diffusion layer is not formed. This weak element diffusion is beneficial to solid-phase welding, which can reduce the distance between different metal atoms and strengthen the solid-phase metallurgical bonding [16]. Geng et al. [28] conducted an electromagnetic pulse welding research and observed that the elemental diffusion of welded joints is an important mechanism of high-speed shock welding.

4.4 Tensile shear test and failure analysis

The brass and SS304-welded samples were subjected to tensile shear failure analysis to measure the quality of welded joints. The effects of different process parameters (laser pulse energy, flight distance, and flyer plate thickness) on the force of the welded joints were studied. Figure 9 shows the schematic of the failure analysis device. Failure analysis involves two failure types, namely, interface peeling failure and joint edge fracture failure, as shown in Fig. 10a and b, respectively. Interface peeling failure mainly occurs when the flight distance or the laser energy is low because the shock velocity obtained by the flyer plate is small, thus forming a flat interface wave shape. Moreover, the two metals have a low joint strength and are easily peeled off during stretching. Joint edge fracture failure occurs because the flyer plate obtains sufficient impact velocity, and the interface gradually becomes a wavy interface. The amplitude and wavelength of the interface wave also decrease as the impact velocity decreases, thereby forming microscopic clamping and ensuring no peeling in the tensile process of the welded joint. In addition, the edge area of the solder joint may cause severe stress concentration due to stretching in the tensile shear test, possibly causing the edge of the solder joint to be broken due to excessive force.

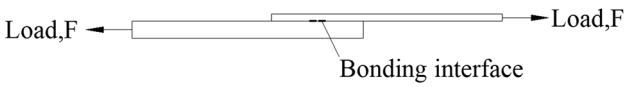

Fig. 9 Schematic diagram of tensile shear failure analysis device

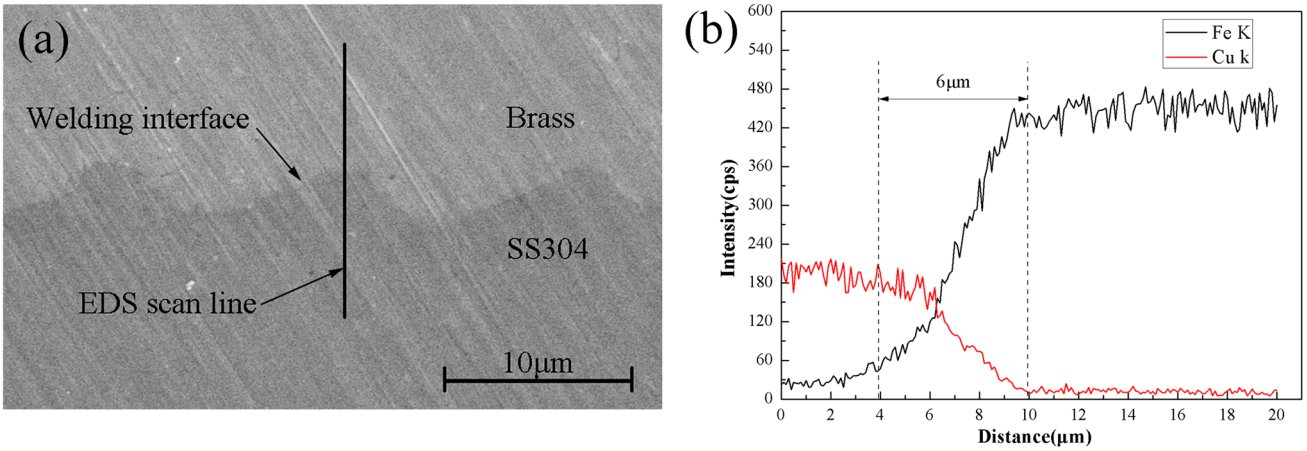

Fig. 8 **a** EDS line scan position of brass/SS304 interface; **b** EDS element line scan result

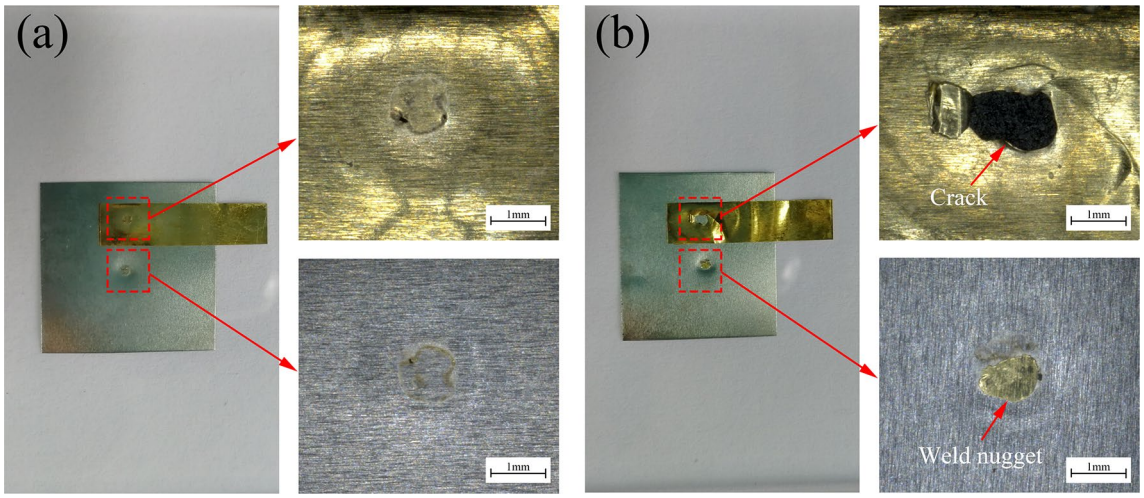

Fig. 10 **a** Peeling failure in bonding interface; **b** Fracture failure on the bonding edge

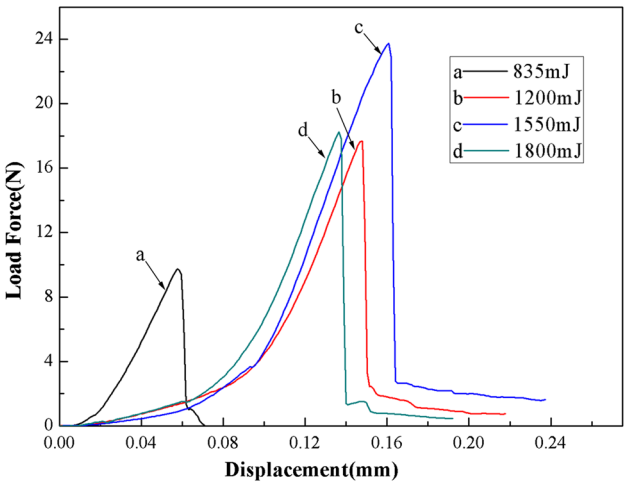

Fig. 11 Force–displacement curves of bonding joints with different laser pulse energies (standoff distance: 0.2 mm; flyer plate thickness: 0.02 mm)

The thickness of the flyer plate (0.02 mm) and the flight distance (0.2 mm) is unchanged during the tensile shear test. As shown in Fig. 11, the curves a, b, c, and d correspond to the force–displacement curves of the bonded joints at 1800, 1550, 1200, and 835 mJ laser energies with maximum forces of 18.26, 23.60, 17.67, and 9.77 N, respectively. The maximum force of the welded joint decreases when the laser pulse energy decreases from 1550 to 835 mJ. The bonding interface between the flyer plate and the substrate has serious plastic deformation under the action of high shear stress and impact pressure. The bonding interface of the welding samples changes from a straight shape to a distinct wave shape as the laser pulse energy increases, thus achieving clamping between the two metals [29]. In addition, the contact area of the interface decreases as the laser energy decrease, thereby indirectly increasing the friction between the bonding interfaces. These factors are beneficial to the increase in the maximum force [30]. Liu et al. [15] found that the effective bonding region increases as laser pulse energy increases. This increase may be the reason for the increase in the maximum force of the bonded joint. However, when the laser pulse energy increases to 1800 mJ, the maximum force is seriously degrades. Considering that the failure mode at 1800 mJ is the fracture failure of the solder joint edge, the thinning of the edge region of the solder joint may be an influencing factor. Figure 12a and b shows the optical microscopic cross sections of solder joint edges with laser pulse energies of 1550 and 1800 mJ, respectively. The thickness of the edge of the solder joint is approximately 0.01846 mm at a laser pulse energy of 1550 mJ. Our calculation reveals that the thinning rate after the impact welding of the flyer plate is 7.7%. When the laser energy increases to 1800 mJ, the thickness of the edge of the solder joint is only 0.01678 mm, and the thinning rate reaches 16.1%, which is much larger than the thinning rate at 1550 mJ. When subjected to force, the flyer plate becomes thinner, and stress is likely produced in the tensile process, leading to the fracture failure of the solder joint edge. The thinning of the edge of the solder joint may be the main reason for the decrease in the bonding strength of the welded sample. Hence, the maximum force decreases at a laser pulse energy of 1800 mJ.

The effects of different flight distances and flyer plate thickness on the tensile strength of the welded samples are studied. The laser pulse energy remains unchanged at 1800 mJ. Tensile shear tests are carried out at thickness–flight distances of the compound plate of 0.02–0.1, 0.02–0.2, 0.02–0.3, 0.03–0.2, and 0.04–0.2 mm. Figure 13 shows the force–displacement curves of the welded joints

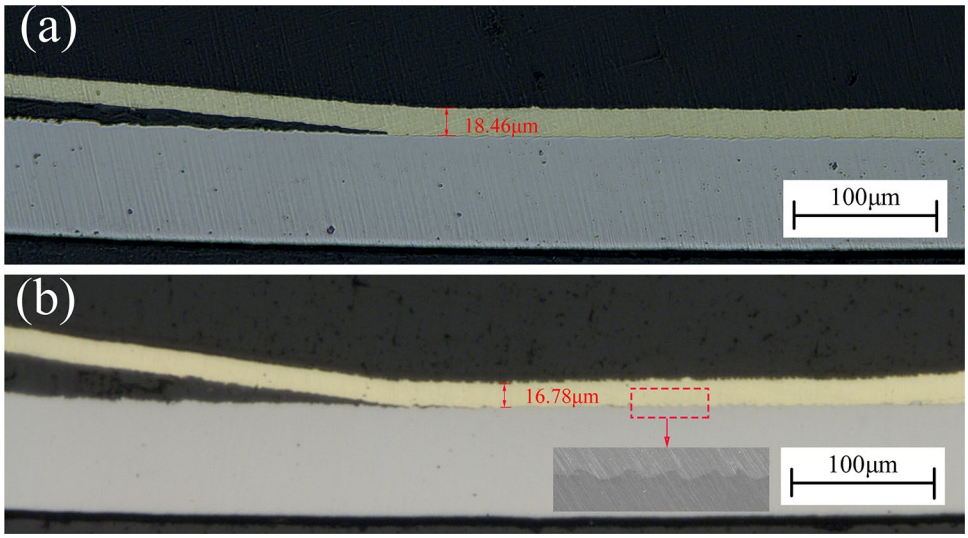

Fig. 12 **a** Thickness of the welding edge (laser pulse energy: 1550 mJ); **b** thickness of the welding edge (laser pulse energy: 1800 mJ)

with curves a, b, and c of the 0.02-mm-thick flyer plate at flight distances of 0.1, 0.2, and 0.3 mm with maximum forces of 12.39, 18.26, and 13.11 N, respectively. The results showed that the maximum force initially increases and then decreases as the flight distance increases. The flight distance between the substrate and flyer plates decreases, so that there is not enough time and distance to accelerate to a higher speed. In addition, the degree of downward bending of the clad plate will decrease with the decrease in the flight distance, and the dynamic impact angle between the substrate and flyer plates is more difficult to reach the critical impact angle in the initial stage of welding. At this time, the collision velocity and collision angle between the flyer and substrate plates are reduced, and the shear stress will also be reduced. The reduction in the shear stress makes the metal surface not easier to peel off and produce jet, which eventually leads to welding failure. At a flying distance of 0.1 mm, the impact velocity is small when the flyer plate hits the substrate. Hence, a wavy bonding interface is not observed, and the bonding strength is relatively small. When the flight distance increases from 0.2 to 0.3 mm, the flyer plate may obtain an increased impact velocity, resulting in increased plastic deformation at the bonding interface. Therefore, the interface waveform size increases, as shown in Figs. 12b and 14a. Durgutlu et al. [31] studied the explosion welding of copper and stainless steel and found that an increase in flight distance can increase the amplitude and wavelength of the interface wave. An increase in the size of the waveform can increase mechanical interlock and friction, and this phenomenon is beneficial to an increase in the force of the welded joint. However, the maximum force at a flight distance of 0.3 mm has been seriously reduced. The welding edge was seriously thinned by the huge impact at a flight distance of 0.3 mm. As shown in Fig. 14a, the thinnest part of the welding joint edge only has a thickness of 0.01–0.03 mm, and the thinning rate reaches 49.85%. When the thinning rate of the welding joint edge is small, the waveform size of the interface wave is the main factor affecting the maximum force. However, when severe thinning occurs, the thinning of the edge region of the welding joint causes more serious stress concentration. When the adverse effect of the thinning of the welding joint edge on the force is greater than the favorable effect caused by the increase in waveform size, the maximum force greatly decreases [22]. Kore et al. [32] examined the electromagnetic pulse welding of aluminum and stainless steel and found that the maximum force initially increases and subsequently decreases as flight distance increases.

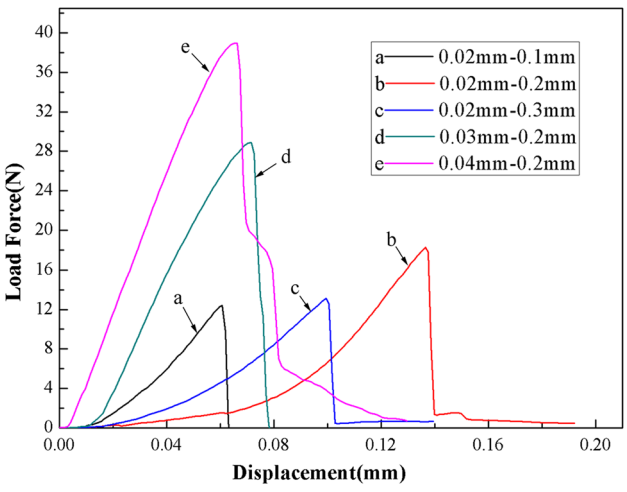

Fig. 13 Force–displacement curves of welding joints with different standoff distances and flyer plate thicknesses (laser pulse energy: 1800 mJ)

The curves b, d, and e in Fig. 13 show the force–displacement curves of the welded joints at flyer plate thicknesses 0.02, 0.03, and 0.04 mm with maximum forces of 18.26,

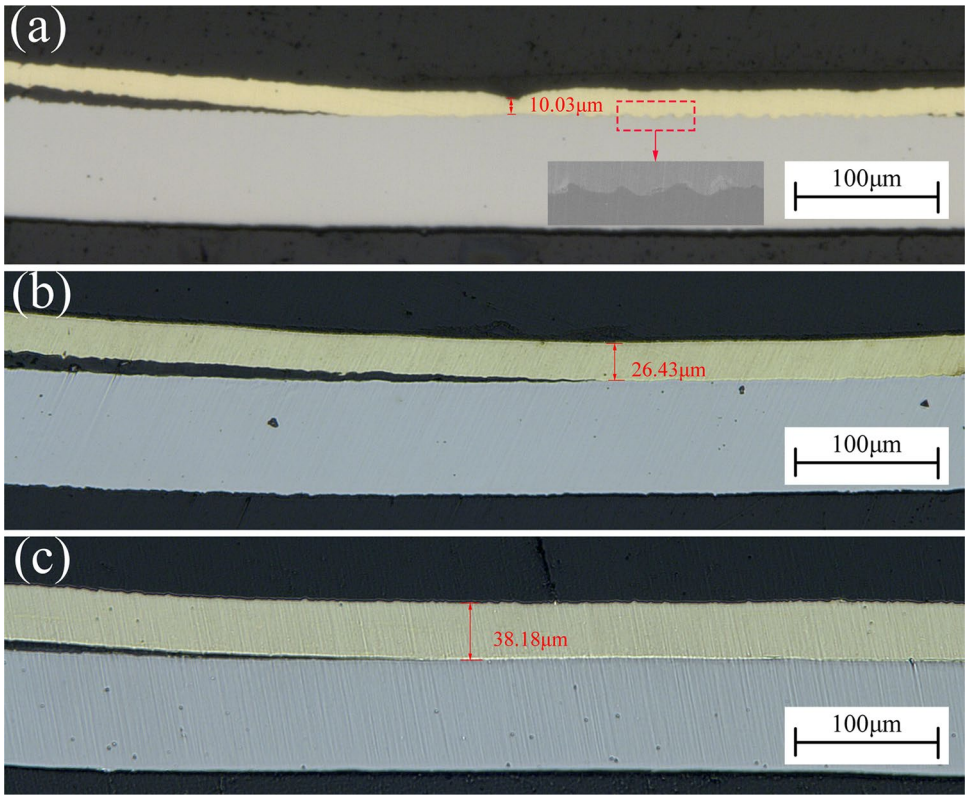

Fig. 14 Thickness of the welding edge: **a** flyer plate thickness of 0.02 mm and flight distance of 0.3 mm; **b** flyer plate thickness of 0.03 mm and flight distance of 0.3 mm; and **c** flyer plate thickness of 0.04 mm and flight distance of 0.3 mm

28.88, and 38.96 N, respectively. The welding strength decreases as the flyer plate thickness decreases because the flyer plate thickness has a wavy-bonded interface with the substrate at a laser energy of 1800 mJ and a flying distance of 0.2 mm, and tensile failure under each thickness value occurs in the form of fracture failure at the welding joint edge. When the flyer plate is thick, a greater force is required for the material to undergo tensile fracture failure due to stress concentration. Although the amplitude and wavelength of the interface waveform decrease as the flyer plate thickness increases, the beneficial effect of the increase in the flyer plate thickness on the maximum force exceeds the adverse effect of the decrease in the amplitude and wavelength of the interface wave. The 0.03-mm- and 0.04-mm-thick flyer plates still have the localized thinning of the welding joint edge during impact welding, as shown in Fig. 14b and c. After LIW, the thicknesses of the welding joint edge of the 0.03-mm- and 0.04-mm-thick flyer plates are reduced to 26.43 and 0.03818 mm, respectively. The thinning rates of the 0.03-mm- and 0.04-mm-thick flyer plates are 11.9%, 4.55%, respectively. The comparison of these rates with the thinning rate of the 0.02-mm-thick flyer plate reveals that thick flyer plates are less prone to thinning. This condition occurs possibly because the thicker the flyer plate is, the smaller the impact velocity will be when the flyer plate collides with the substrate plate, resulting in the plastic deformation of the flyer plate and producing a relatively small substrate. Hence, the flyer plate does not cause serious thinning.

5 Conclusion

Brass and stainless steel were successfully welded by LIW. The effects of flight distance, laser pulse energy, and plate thickness on the welding of the two alloys were investigated. The effects of flyer plate thickness and laser pulse energy on the surface morphology and micromorphology of the welding samples were also studied, and elemental diffusion at the welding interface was analyzed. The influences of the laser energy, flight distance, and thickness of the flyer plate on the force were discussed. The main results were as follows:

(1) When the laser pulse energy is 1200 mJ, the surface of the bonding specimen is flat and smooth. When the laser energy is increased to 1800 mJ, ripples are observed on the surface of the flyer plate. When the flyer plate thickness is constant, the effective welding area decreases as the laser pulse energy decreases, whereas the effective welding area decreases as the flyer plate thickness increases.
(2) Under the flying distance of 0.2 mm, when the flyer plate thickness is constant, the amplitude and wavelength of the interface wave decrease as the laser pulse

energy decrease. However, the amplitude and wavelength of the interface wave decrease as the flyer plate thickness increases under the same laser pulse energy and still produces a wavy interface. EDS analysis results show an approximately 6-μm-thick elemental diffusion layer at the bonding interface.

(3) Two failure modes, namely, peeling failure of the bonding interface and fracture failure of the bonding joint edge, occur in the failure analysis. The bonding interface peeling failure occurs only when the laser energy is 565 mJ or the flight distance is 0.1 mm, whereas the failure mode is the fracture failure of the welding joint edge under other welding conditions.

(4) When the thickness of the flyer plate is 0.02 mm under the excessive laser energy or flight distance, the edge of the welding joint becomes thinner and more severe. The results show that the welding strength is simultaneously affected by the waveform size of the bonding interface and the thinning of the welding joint edge flyer plate. When the laser energy and the flight distance are constant, the flyer plate is, the smaller the thinning rate will be. The welding strength decreases as the flyer plate thickness decreases.

Acknowledgements This work is supported by the National Natural Science Foundation of China (NO.51675241).

References

1. Yang JN, Zhang LJ, Ning J, Bai QL, Yin XQ, Zhang JX (2017) Single pass laser-MIG hybrid welding of 8-mm thick pure copper (T2) without preheating: microstructure and properties. Appl Therm Eng 126:867–883
2. Li Y, Hu SS, Shen JQ, Liu LL (2015) Microstructures and mechanical properties of H62 brass-316L stainless steel in overlap welded joints by continuous-wave laser. Int J Adv Manuf Technol 79:627–634
3. Cao J, Zhang LX, Wang HQ, Wu LZ, Feng JC (2011) Effect of silver content on microstructure and properties of brass/steel induction brazing joint using Ag-Cu-Zn-Sn filler metal. J Mater Sci Technol 7:377–381
4. Liu BX, Huang LJ, Geng L, Wang B, Liu C, Zhang WC (2014) Fabrication and superior ductility of laminated Ti-TiBw/Ti flyers by diffusion welding. J Alloy Compd 602:187–192
5. Wronka B (2011) Testing of explosive welding and welded joints. Wavy character of the process and joint quality. Int J Impact Eng 38:309–313
6. Luo J, Xiang JF, Liu DJ, Li F, Xue KL (2012) Radial friction welding interface between brass and high carbon steel. J Mater Process Technol 212:385–392
7. Kimura M, Kasuya K, Kusaka M, Kaizu K, Fuji A (2013) Effect of friction welding condition on joining phenomena and joint strength of friction welded joint between brass and low carbon steel. Sci Technol Weld Join 14:404–412
8. Bai QL, Zhang LJ, Xie MX, Yang HX, Zhang JX (2016) An investigation into the inhomogeneity of the microstructure and mechanical properties of explosive welded H62-brass/Q235B-steel clad plates. Int J Adv Manuf Technol 90:1351–1363
9. Gao Y, Nakata K, Nagatsuka K, Matsuyama T, Shibata Y, Amano M (2016) Microstructures and mechanical properties of friction stir welded brass/steel dissimilar lap joints at various welding speeds. Mater Des 90:1018–1025
10. Angshuman K, Abhay S (2015) Magnetic pulse welding: an efficient and environmentally friendly multi-material joining technique. J Clean Prod 100:35–58
11. Zhang Y, Babu SS, Prothe C, Blakely M, Kwasegroch J, Laha M, Daehn GS (2011) Application of high velocity impact welding at varied different length scales. J Mater Process Technol 211:944–952
12. Wang X, Gu CX, Zheng YY, Shen ZB, Liu HX (2014) Laser shock welding of aluminum/aluminum and aluminum/copper plates. Mater Des 56:26–30
13. Wang HM, Taber G, Liu DJ, Hansen S, Chowdhury E, Terry S, Lippold JC, Daehn GS (2015) Laser impact welding: design of apparatus and parametric optimization. J Manuf Process 19:118–124
14. Wang HM, Vivek A, Wang YL, Taber G, Daehn GS (2016) Laser impact welding application in joining aluminum to titanium. J Laser Appl 28:032002
15. Liu HX, Gao S, Yan Z, Li LY, Li C, Sun XQ, Sha CF, Shen ZB, Ma YJ, Wang X (2016) Investigation on a novel laser impact spot welding. Metals 6:179
16. Wang X, Huang T, Luo YP, Liu HX (2017) Laser indirect shock welding of fine wire to metal sheet. Materials. https://doi.org/10.3390/ma10091070
17. Liu HX, Jin H, Shao M, Tang H, Wang X (2018) Investigation on interface morphology and mechanical properties of three-layer laser impact welding of Cu/Al/Cu. Metall Mater Trans A-Phys Metall Mater Sci 50:1273–1282
18. Wang X, Luo YP, Huang T, Liu HX (2017) Experimental investigation on laser impact welding of Fe-based amorphous alloys to crystalline copper. Materials. https://doi.org/10.3390/ma10050523
19. Wang X, Shao M, Jin H, Tang H, Liu HX (2019) Laser impact welding of aluminum to brass. J Mater Process Technol 269:190–199
20. Wang X, Gu YX, Qiu TB, Ma YJ, Zhang D, Liu HX (2015) An experimental and numerical study of laser impact spot welding. Mater Des 65:1143–1152
21. Zheng YM (2007) The principle and application of explosive welding and metallic composite. Central South University Press, Changsha **(in Chinese)**
22. Wang X, Li F, Huang T, Wang XJ, Liu HX (2019) Experimental and numerical study on the laser shock welding of aluminum to stainless steel. Opt Lasers Eng 115:74–85
23. Kahraman N, Gülenç B (2005) Microstructural and mechanical properties of Cu–Ti plates bonded through explosive welding process. J Mater Process Technol 169:67–71
24. Acarer M, Gülenç B, Findik F (2003) Investigation of explosive welding parameters and their effects on microhardness and shear strength. Mater Des 24:659–664
25. Chen PW, Feng JR, Zhou Q, An EF, Li JB, Yuan Y, Ou SL (2016) Investigation on the explosive welding of 1100 aluminum alloy and AZ31 magnesium alloy. J Mater Eng Perform 25:2635–2641
26. Mousavi SAAA, Sartangi PF (2009) Experimental investigation of explosive welding of cp-titanium/AISI 304 stainless steel. Mater Des 30:459–468
27. Akbari-Mousavi SAA, Barrett LM, Al-Hassani STS (2008) Explosive welding of metal plates. J Mater Process Technol 202:224–239
28. Geng HH, Xia ZH, Zhang X, Li GY, Cui JJ (2018) Microstructures and mechanical properties of the welded AA5182/HC340LA joint by magnetic pulse welding. Mater Charact 138:229–237

29. Jiang MQ, Huang BM, Jiang ZJ, Lu C, Dai LH (2015) Joining of bulk metallic glass to brass by thick-walled cylinder explosion. Scr Mater 97:17–20
30. Borchers C, Lenz M, Deutges M, Klein H, Gartner F, Hammerschmidt M, Kreye H (2016) Microstructure and mechanical properties of medium-carbon steel bonded on low-carbon steel by explosive welding. Mater Des 89:369–376
31. Durgutlu A, Okuyucu H, Gulenc B (2008) Investigation of effect of the stand-off distance on interface characteristics of explosively welded copper and stainless steel. Mater Des 29:1480–1484
32. Kore SD, Date PP, Kulkarni SV (2008) Electromagnetic impact welding of aluminum to stainless steel sheets. J Mater Process Technol 208:486–493